USE OF LAGRANGIAN SIMULATIONS TO HINDCAST THE GEOGRAPHICAL POSITION OF PROPAGULE RELEASE ZONES IN A MEDITERRANEAN COASTAL FISH

Antonio Calò[1,4]*, Christophe Lett[2,5], Baptiste Mourre[3], Ángel Pérez-Ruzafa[1], José Antonio García-Charton[1]

[1]Departamento de Ecología e Hidrología, Universidad de Murcia, Campus Espinardo, 30100, Murcia, Spain;

[2]Sorbonne Universités, UPMC Univ Paris06, IRD, unité de modélisation mathématique et informatique des systèmes complexes (UMMISCO), F-93143, Bondy, France;

[3]Modelling and Forecasting facility, Balearic Islands Coastal Observing and Forecasting System (SOCIB), Palma, Balearic Islands, Spain;

[4]Present address: Université Nice Sophia Antipolis, CNRS, FRE 3729 ECOMERS, Parc Valrose 28, 06108 Nice Cedex, France

[5]Present address: UMR MARBEC, Station Ifremer de Sète, Avenue J. Monnet, 34203 Sète Cedex, France

*antoniocalo.es@gmail.com

ABSTRACT

The study of organism dispersal is fundamental for elucidating patterns of connectivity between populations, thus crucial for the design of effective protection and management strategies. This is especially challenging in the case of coastal fish, for which information on egg release zones (i.e. spawning grounds) is often lacking. Here we assessed the putative location of egg release zones of the saddled sea bream (*Oblada melanura)* along the south-eastern coast of Spain in 2013. To this aim, we hindcasted propagule (egg and larva) dispersal using Lagrangian simulations with two approaches: 1) back-tracking and 2) comparing settler distribution obtained from simulations to the analogous distribution resulting from otolith chemical analysis. Simulations were also used to

assess which factors contributed the most to dispersal distances. In back-tracking simulations, the majority of particles were moved back in time southward, suggesting that the North-African coasts and the Easter Alboran Sea were hydrodynamically suitable to generate and drive the supply of larvae along the coast of Murcia. With the second approach, a correlation between simulation outputs and field results (otolith chemical analysis) was found, suggesting that the oceanographic characteristics of the study area could have determined the pattern of settler distribution recorded with otolith analysis in 2013. Dispersal distance was found to be significantly affected by the geographical position of propagule release zones. The combination of methods used was the first attempt to assess the geographical position of propagule release zones in the Mediterranean Sea for *O. melanura*, and can represent a valuable approach for elucidating dispersal and connectivity patterns in other coastal species.

INTRODUCTION

The study of causes and consequences of organism dispersal is crucial from both ecological and evolutionary perspectives (Burgess et al., 2015). It provides vital information on demographic processes, species responses to environmental variability and anthropogenic stresses and on gene flow among populations, which, in turn, affect meta-population dynamics and species local adaptation (Burgess et al., 2015). In the case of fish, dispersal plays a major role in determining the spatial scale over which populations interact genetically and ecologically (i.e. connectivity) and how they should be managed (Grüss et al., 2011; Green et al., 2014). In spite of its great importance, the quantification of dispersal is still a challenging issue. Direct measures of dispersal are made hard by the difficulty to track individuals throughout their life cycle, especially during early developmental stages (Barbee and Swearer, 2007; Cowen, 2007; Calò et al., 2013). Most marine coastal fish species have a complex life cycle including a pelagic propagule (egg and/or larva) phase, that ends with the settlement in benthic habitats, followed by a demersal juvenile/adult phase (Leis et al., 2011). For these fishes, post-settlement stages are considered relatively site attached, so it is the propagule phase that contributes mostly to species dispersal capacity (Leis, 2015), although, in some cases, movement by juveniles (Di Franco et al., 2015) and adults (Aspillaga et al., 2016) can significantly contribute to population connectivity. In this context, a major issue for fish ecologists is the lack of knowledge on the locations where eggs are released (i.e. spawning grounds) (Thorrold et al., 2007). This, together with the minuscule dimension of eggs and larvae, makes it impractical to track propagules from their origins to their destination (i.e. settlement sites) and obtain an exhaustive measure of connectivity during the pelagic phase (Thorrold et al., 2001). The location of egg release zones is only possible through direct observations of spawning events or using acoustic methods, or indirectly through traditional ecological knowledge (e.g. fisherman knowledge about zones of fish massive catches) (Heyman et al., 2004; Boomhower et al., 2007).

In the last decades, modelling tools based on outputs of water circulation models were developed to simulate particle dispersal. Assuming that propagules are advected and diffused similarly to water particles (Cowen, 2007), Lagrangian-based, spatially-explicit individual-based models (IBMs) have been recognized as powerful tools to track pelagic particles from potential release zones to settlement habitats (Werner et al., 2007; Watson et al., 2010). IBMs have been used both to hindcast and forecast patterns of propagule transport and address challenging ecological questions such as: the assessment of the potential impact of climate change on propagule dispersal (Lett et al., 2010; Andrello et al., 2015b) or to help in the design of MPA networks and in their future management (Andrello et al., 2015a; Andrello et al., 2017). IBMs have been also used to understand how

82 dispersal and connectivity can be influenced by spatial and temporal variability of different physical

83 and biological factors (Andrello et al., 2013; Ospina-Álvarez et al., 2013; Ospina-Alvarez et al.,

84 2015; Tanner et al., 2017), providing crucial information on the factors that drive fish settlement

85 variability and giving support to the development of effective fishery management strategies

86 (Ospina-Alvarez et al., 2015). Model simulations were also used to corroborate results or test

87 hypotheses on propagule dispersal based on complementary methodologies such as genetic analysis

88 or chemical analysis of calcified structures (e.g. (Calò et al., 2013), in the Mediterranean Sea).

89 In 2013, otoliths of juvenile individuals of the saddled sea bream (*Oblada melanura*) were analysed

90 chemically to identify the number of potential natal sources along the Mediterranean south-eastern

91 coast of Spain (Murcia region). A set of release zones were found to supply a series of coastal sites

92 spread along ~180 km of coastline (Calò et al., 2016). Otolith analysis does not allow to assess the

93 geographical position of natal origins. In this context, dispersal simulations could be used to

94 hindcast the position of the propagules' sources previously identified.

95 In the present study we implemented a biophysical IBM to investigate the putative geographical

96 position of propagule release zones of *Oblada melanura* previously discriminated with otolith

97 chemical analysis, along the south-eastern coast of Spain in 2013. Dispersal simulations were also

98 used to assess the factors more likely to influence propagule dispersal distances in the region. We

99 used species-specific information on early life history traits (ELTs), i.e. spawning dates, pelagic

100 larval duration and settlement dates, of the selected species. This information was gathered in the

101 same spatial and temporal context of the oceanographic data implemented for the simulations. Apart

102 from their ecological importance in the geographic context considered, the results of the study can

103 provide useful insights for the development of new approaches to investigate the location of fish

104 spawning areas.

MATERIAL AND METHODS

Hydrodynamic model

The Western Mediterranean OPerational forecasting system (WMOP, (Juza et al., 2016)) is based on a regional ocean configuration of the ROMS model implemented over the Western Mediterranean Sea (www.socib.es). The ROMS is a free-surface split-explicit model, solving the hydrostatic primitive equations using terrain-following curvilinear vertical coordinates, employing the Arakawa-C horizontal and vertical grid staggering (Shchepetkin and McWilliams, 2005). The WMOP has a horizontal resolution from 1.8 to 2.2 km and 32 sigma-levels in the vertical dimension, with a spatial coverage from Gibraltar strait to Sardinia Channel (6ºW, 9ºE, 35ºN, 44.5ºN). The model is forced by high-resolution winds (5 km, 3 hours) from the Spanish Meteorological Agency. The simulation used in this study is a sample over the period 2013-2014 of a 6.5-year long simulation of WMOP starting in September 2008. Initial and boundary conditions were provided by the CMEMS MED-MFC model.

Larval dispersal model

Daily outputs of three-dimensional velocities fields simulated by WMOP were used to simulate *Oblada melanura* larval dispersal using the software Ichthyop 3.2 (Lett et al., 2008). The time step of larval transport was set to 100 s in order to keep it lower than the ratio of cell size to maximum current velocity, so that propagules do not cross more than one cell boundary in a single time step (Courant–Friedrichs–Lewy condition). Given that no information on egg buoyancy nor larval active swimming and vertical migration are available for *O. melanura*, in all the simulations a neutral buoyancy was assigned to eggs and larvae, which were subjected only to current transport (i.e. passive dispersal).

Putative natal origins and settler distribution of Oblada melanura

To locate the major natal origins of *O. melaura* identified along the study area in 2013, two different approaches were used: 1) backtracking propagule dispersal simulations and 2) the comparison between settler distributions obtained from forward model simulations and the pattern recorded from post-settler otolith chemistry by (Calò et al., 2016)).

Running the larval dispersal model in backtracking mode allowed to explore those areas where it was hydrodynamically possible for propagules to be transported toward the coastal sites in which juveniles were sampled in 2013. Micro-structural analyses performed on the otoliths of pre-settlers individuals of *O. melanura* (i.e. larval individuals, sampled close to the coast, that are in the last phase of larval phase) indicated that the mean age of larvae (days after hatching), immediately

140 before settlement, was 11.5 days in 2013 (Calò et al. unpublished data). This measure of larval

141 duration was 2 days shorter than the standard pelagic larval duration (PLD) as measured with the

142 analysis of otoliths of individuals that had already settled. For this reason, the dispersal duration

143 used for the backtracking simulation was 13.5 days, i.e. the sum of the mean days after hatching

144 plus 2 days of egg phase duration. The choice to use a shorter measure of larval duration was made

145 in order to exclude the last days of larval life (i.e. the competency phase) in which behavioural and

146 movement capabilities are likely developed (Leis, 2007). Moreover, shortening the dispersal

147 duration has proven to determine similar effects to introducing some larval behaviour in the model,

148 reducing the effect of considering propagules as passive particles (Andrello et al., 2013) (Andrello

149 et al., 2017). In backward simulations, particles released from a backward-time-release-zone started

150 their 'virtual life' with a positive age (i.e. 13.5 days) and became younger as the simulation moves

151 towards completion (as simulated time retreats/regresses). Nine backward-time-release-zones were

152 distributed along the coast, in correspondence to the locations where settlers were sampled in 2013

153 for otolith chemical analysis (Figs 1a and b). Particles were released following the settlement dates

154 of *O. melanura* recorded in 2013. Eight simulations were run covering all sampled dates moving

155 backward in time from July 14th to July 7th. In each simulation 1,000 particles were released from

156 each backward-release-zone, a number which was initially tested as being large enough to cover all

157 possible origins of the particles.

158 For the second approach, the settler distribution recorded along the coast in 2013, as resulted from

159 otolith chemical analyses (Calò et al., 2016), was tested against a series of settler distributions

160 resulting from different Ichthyop runs. In these forward simulations, particles released from

161 forward-time-release-zones started their 'virtual life' with age=0 and grow older as the simulation

162 moves towards completion (as simulated time progresses/advances). In each model run, forward-

163 release-zones were randomly selected from a set of potential release zones distributed along the

164 coast. Previous results from otolith chemical analyses (Calò et al, 2016) showed the presence of 5

165 major natal origins (here considered as a proxy of egg release zones) that supplied 17 coastal sites

166 in 2013. In order to compare these results with Ichthyop simulation outputs, settler distribution data

167 from the 17 sites were pooled, by couples of neighbouring sites, into 9 locations (apart from site 7,

168 Fig. 1a and b). In Ichthyop, 13 potential release zones were created: 9 were located in

169 correspondence to the 9 'pooled locations' of the otolith study (named from L1 to L9, Fig. 1b), 2

170 zones were located immediately outside the sampled area (O1 and O2) and 2 other zones were

171 positioned inside the study area (M1 and M2). These last 4 zones were created for better covering

172 the whole domain. The zones L1-L9 (Fig. 1b) were used as settlement zones (the same 9 zones

173 being used in the backtracking experiment). All the release and settlement zones had the same

174 surface. Fifty Ichthyop simulations (of the possible 1287) were run, each with 5 release zones

175 randomly selected from the set of 13 potential release zones. The duration of dispersal phase used

176 for running the model was the mean 13.5 days, as for backward simulations. In all simulations, we

177 considered a spawning depth range of 0-20 m, which is where larvae of *O. melanura* are more

178 commonly found (Sabatés et al., 2007). The spawning dates recorded for *O. melanura* in 2013

179 (from June 21th to July 2nd), were used for daily release, accounting for 95% of all the spawning

180 dates recorded in 2013 (Calò et al unpublished data). Two hundred particles were released for each

181 zone and date, for a total of 12,000 particles per simulation (200 particles × 5 zones × 12 dates). In

182 Ichthyop the 'stop when recruited' option was turned on, i.e. particles were assumed to settle and

183 stop moving when passing over a settlement zone, and considering a minimum age for settling of 10

184 days, that was the minimum age found for pre-settlement individuals of *O.melanura* in 2013 (Calò

185 et al unpublished data). After each model run, the distribution of propagules that settled in the 9

186 settlement zones was used to generate a data frame with 5 variables (release zones) and 9 replicates

187 (settlement zones). Each value of the data frame represented the ratio of propagules settled in one of

188 the 9 settlement zones, released from each of the 5 random release zones, divided by the total

189 number of settling propagules from each release zone. A Mantel's test based on 10^6 permutations

190 (performed with 'ade4' package, R software) was used to investigate which model-generated settler

191 distributions were significantly correlated to the analogous distribution obtained from otolith

192 analysis (built with the 5 major natal origins and the 9 'pooled locations'). Before performing

193 Mantel's tests, a distance matrix (based on Euclidean distance) was created from each data frame.

194 After the first 50 simulations, the release zones that produced statistically significant Mantel's tests

195 (8 of the original 13, see Results) were used for running new Ichthyop runs with the same

196 simulation settings as before but covering all the 56 possible combinations of 5 natal sources (in the

197 possible 8). Simulation outputs were tested against the data frame resulting from otolith analysis

198 using Mantel's test as described above.

199 Finally patterns of settler distributions generated from simulations that produced statistically

200 significant Mantel's tests were analysed and compared to the pattern recorded from otolith chemical

201 analysis. For model-generated settler distributions, the local retention, defined as the fraction of

202 propagules released from a zone that settled back to the same zone, was also assessed.

203

204 *Dispersal distance of Oblada melanura*

205 To investigate the factors contributing to propagule dispersal of *O. melanura* along the coast of the

206 Murcia region, the distance from the release point to the final point at the end of larval transport

207 was measured for each simulated larva as the great-circle distance (i.e. the shortest distance between

208 two points on a sphere). Three release zones were selected from the set of 13 release zones

209 previously considered in the forward simulations: L1 , L5 and M2 respectively in the north, centre

210   and south of the study area. These zones host three MPAs of the region, respectively from north to
211   south: Tabarca MPA (established in 1986), Cabo de Palos MPA (established in 1995) and Cabo
212   Tiñoso MPA (established in 2016). Given that no information on the exact spawning depth range of
213   *O. melanura* is available, we considered 4 different release depth ranges: 0-5 m, 5-10m, 10-15m
214   and 15-20m. Two different propagule dispersal durations were considered as resulted from otolith
215   micro-structural analysis: the mean days after hatching (11.5 days), i.e. the mean larval duration
216   recorded for larvae sampled close to the coast immediately after settlement, and the mean PLD (14
217   days), i.e. the measure of larval duration recorded for individuals that had already settled. An
218   Ichthyop simulation was run for each combination of depth ranges (4) and dispersal durations (2),
219   resulting in a total of 8 runs. In each run 30 particles were released in each of the 3 release zones
220   and following the spawning period recorded in *O. melanura* in 2013, i.e. from June 21th to July 2nd
221   for a total of 12 releasing dates. A high consistency between simulation runs repeated under the
222   same software configuration and parameter values was observed during preliminary analyses,
223   indicating that the number of released particles was sufficient to provide robust simulated patterns.
224   Model outputs were merged together creating a data frame containing 720 dispersal distance values
225   (4 depth ranges × 2 dispersal durations × 3 zones × 30 particles). To test for potential differences in
226   dispersal distances related to the position of the spawning zone, depth and the duration of propagule
227   dispersal phase, an analysis of variance (ANOVA) was performed, considering the factors 'Release
228   zone' (Z) (random, with 3 levels), 'Depth range' (D) (fixed, with 4 levels crossed to Z), and
229   'Dispersal duration time' (T) (fixed, with 2 levels, PLD *vs*. DAH, crossed to Z and D). There were
230   30 replicate distance values (one for each simulated propagule) per each combination of levels of
231   the three factors considered. Before performing ANOVA, data were tested for homogeneity of
232   variance using Chocran's test, finding no evidence of heterogeneity of variance in all cases
233   (p>0.05). ANOVA was run using the GAD package in R software (R Development Core Team,
234   2013).

RESULTS

Putative natal origins and settler distribution of Oblada melanura

Backward simulations showed that most particles were transported southward (Fig. 2). Nevertheless, in two simulations, corresponding to the release dates 14th and 13th of July, an inshore accumulation of propagules was recorded along a stripe between release zones 2 and 4, in the north of the study area (Figs. 2 a and b). In both cases these particles originated from backward-time-release-zone L3. In two other simulations (release dates 10th and 9th of July, Figs. 2 e and f), an inshore accumulation of propagules, also originated from backward-time-release-zone L3, was observed in the north of the study area, in proximity of Tabarca MPA.

Concerning forward simulations from randomly selected sets of forward-release zones (second approach), the 5 random release zones selected for each of the first 50 model runs and the associated Mantel's tests are reported in Table S1 (Supplementary Material). Among all Mantel's tests performed between the settler distribution resulting from otolith chemical analysis and the Ichthyop-generated settler distributions, two tests (Ichthyop runs #3 and #28) were statistically significant ($p < 0.05$), indicating a correlation between field data and model simulation outputs (Table S1, Supplementary Material). The forward-release zones that produced these 2 statistically significant Mantel's tests (O1, L1, L2, L3, L5, M2, L9 and O2) were combined in sets of 5 and used for the second group of 56 model runs (thus, release zones M1, L4, L6, L7 and L8 were excluded from the second set of simulations). From this second group of simulations, 8 new runs (out of 10, considering the previous two) produced settler distributions significantly correlated (Mantel's test: $p < 0.05$) to the analogous settler distribution resulting from otolith chemical analysis (Table S2, Supplementary Material).

For these 10 runs, the settler distribution in the 9 'pooled locations' from the 5 major natal origins are shown in Fig. 3b-k aside the distribution resulted from otolith chemical analysis (Fig. 3a). Release zones L2 and O2 were present 9 times; zones O1, L1, L5, M2, L9 were present from 5 to 7 times; while L3 was present 3 times (Fig. 3 b-k). Considering these 10 simulations, the mean percentage of local retention was 29.9% (average from release zones L1 to L9 over all dates), with the highest values (46.3%) recorded in L2 and the minimum (1.2%) recorded in L5. Propagules released from L2 supplied almost all the settlement zones considered. Propagules released in L2 settled predominantly within L2 (i.e., were retained locally) and settlement decreased in areas with increasing distance from L2 (Fig 3b, d, e, f, j, k). The same pattern applies to L3 and L9 (except Fig. 3e). Simulated settled propagule distribution was different between the northern and the southern sector of the study area, with release zones in the north (O1, L1, L2, and L3) only supplying the northern and the central settlement zones while the opposite was observed for

270   propagules released from the southern zones (L5, M2, L9, O2; Fig. 3).

271

272   *Dispersal distance of Oblada melanura*

273   Simulated dispersal distances ranged from 1 to 197 km with a mean value of 55.2 km considering

274   all model runs. Short dispersal distances were more common than longer ones: 62% dispersed

275   between 0 and 50 km, 17% between 50 and 100km, 15% between 100 and 150km and 6% between

276   150 and 200 km (Fig. 4). A significant interaction between factors 'Z' (release zone) and 'D' (depth

277   range) was detected (Table 1), so that the effect of depth on dispersal distances depended on the

278   release zone. Indeed, for the three selected zones, dispersal distance tended to increase with depth,

279   but this increase was strong in Tabarca, weak in Cabo Tiñoso, whereas in the case of Cabo de Palos

280   a difference in dispersal distance was only found between the shallowest depth level (0-5 m) and the

281   others (Fig. 5). Overall, distances obtained for particles released in Cabo de Palos (88.2 ± 3.1 km,

282   mean ± SE) were greater than for those released from Tabarca (44.2 ± 2.8km) and from Cabo

283   Tiñoso (33.1 ± 1.8km) (Fig. 5). No effect of dispersal duration was found in the range of tested

284   values (Table 1).

DISCUSSION

The geographical location of fish propagule release zones is considered by fish ecologists as one of the hardest issues to solve. Here we adopted two approaches to hindcast the putative location of *O. melanura* propagule release zones along the coast of the Murcia region.

The first approach (back-ward simulations) was used to assess which zones had the optimal hydrodynamic characteristics to originate and drive the supply of larvae sampled in 2013. Simulations conducted backward in time showed that the majority of propagules could have originated in areas tens of kilometres southward. The transport of particles towards the southern sector of the Alboran Sea suggests that the North-African coast could potentially host spawning grounds of *O. melanura*. From this perspective, the distance between the Algerian coast and the south-eastern Spanish coast (150-200 km) is comparable to the distance that the saddled sea bream is able to cover during the propagule phase (Calò et al, 2016). In some backward simulations, a portion of propagules was moved back in time toward coastal areas that can potentially sustain adult populations of *O. melanura*., in particular the northern sector of the study area, from zone L4 to zone L2 (Tabarca marine reserve). These zones are characterised by extended patches of sea grass beds (mainly composed by *Posidonia oceanica*) disposed along the coast (Sánchez-Lisazo, 1993); (Calvin Calvo et al., 1999) that represent optimal habitats for hosting reproductive populations of saddled sea bream. Moreover, in the absence of any information on the reproductive habits of the saddled sea bream it is not possible to exclude *a priori* that offshore sectors of the Eastern Alboran Sea could host reproductive grounds of this species.

In the second approach, we considered the set of natal origins discriminated by otolith chemical analysis of juvenile individuals collected in 2013 (Calò et al., 2016) and evaluated their putative geographical position along the study area. The results showed that ten simulations, run using different sets of release zones, produced settled propagule distributions that were significantly correlated to the analogous observed settler distribution. Generally, these simulations included similar release zones, with 2 zones (L2 and O2) present in almost all the simulations, demonstrating consistency among model outputs.

In the simulated propagule distributions, for most release zones, the fraction of settled propagules was highest in the zone itself and decreased with increasing distance from each zone. This pattern is in agreement with the spatial correlation among frequencies of settlers sharing the same natal origin observed in (Calò et al., 2016). The identification of the exact geographical position of the natal origins found with otolith chemical analysis is extremely difficult using currently available methodologies. Thus, it is hard to establish whether the spatial dependency characterising settler frequencies found in (Calò et al., 2016) is the consequence of a distance-dependent dispersal from

the spawning areas. However, the concordance with simulation outputs allows us to hypothesize the putative position of the natal origins identified from otolith analysis. For model-generated distributions, the highest fraction of settled propagules was generally recorded inside or in the proximity of the corresponding release zone: for the release zones L2 (Tabarca marine reserve), L3 and L9 the highest fraction of settled propagules corresponded to local retention, while in the case of O1, M2 (Cabo Tiñoso MPA) and O2 the highest fraction settled in the closest zone. Only in the case of L1 and L5 (Cabo de Palos marine reserve) a partial southward shift was recorded between the release zones and the settlement zones where the highest frequencies of settling propagules were recorded. These results suggest that, in certain sectors of the study area, the pattern of currents could have promoted a distance-dependent dispersal from release zones, with short dispersal distances more likely to occur than longer ones. From these considerations, we speculate that some of the main natal origins identified in juvenile individuals caught in 2013, based on otolith micro-chemistry, could have been located inside or in proximity of the zones where the highest fractions of settlers were recorded. Release zone L2 (Tabarca island) could be of critical importance for *O. melanura* in the region considered as it was present in almost all model simulations that produced significant correlations with otolith results, and it was also the zone supplying the majority of settlement zones. Concurrently, in this zone the highest frequency of settlers sharing the same natal origin was recorded (Fig. 3a). As stated before, this zone was also identified in the backward simulations. Therefore, zone L2 could likely host one of the natal origins identified with otolith analysis. Noticeably, this zone hosts the marine reserve of Tabarca, an effective MPA (Lozano Quijada and Ramos-Esplá, 2015), with coastal habitats mainly characterised by shallow rocky bottoms and *P. oceanica* sea grass beds (Ramos-Esplá, 1985). Propagule distribution from model simulations also showed a clear separation between the northern and the southern sectors of the study area: propagules released from northern zones rarely reached settlement zones in the south of the study area and *vice versa*. This outcome is concordant with the significant difference in settler natal origin composition identified between the two sectors, using otolith chemical analysis (Calò et al., 2016). The resemblance between simulation outputs and field results from otolith analysis suggests that small and mesoscale oceanographic features, like coastal eddies, could have played a major role in shaping settler distribution of *O. melanura* along the study area. The formation of mesoscale eddies (MEs, with a diameter of 50-100 km) is frequent along the stretch of coastline considered (Millot, 1999), and was also observed in the simulations carried out in this study. Recent studies highlighted that MEs may represent important habitats for the larval stages of coastal fishes, due to increased primary and secondary productivity (Nakata et al., 2000) (Sabatés et al., 2007) (Shulzitski et al., 2015) (Sabatés et al., 2013). There are evidences that larvae entering MEs grow consistently faster than those outside the eddies, consequently leading to lower mortality rates and

higher successful settlement in coastal habitats (Shulzitski et al., 2015). MEs could also be responsible for larval patch formation in the pelagic environment, supporting the results on patch cohesiveness recorded in the study area, based on otolith analysis of larvae (Calò et al, 2016) consisting in that groups of larvae originating from different natal origins could merge during their larval phase. From this perspective, even in the absence of behavioural traits or active movements, the formation of heterogeneous larval patches can be promoted by water mixing structures in different moments of the pelagic phase. In the model implemented here, we considered larvae as passive particles, including no behavioural or movement capabilities, thus potentially biasing our model outputs (Leis, 2007) (Leis et al., 2011). On the other hand, by shortening the dispersal duration implemented (i.e. using the DAH instead of the PLD) we prevented running the model during the competency phase of the saddled sea bream (Calò et al. unpublished data), thus reducing the potential influence of behaviour and active movements that characterise the last moment of the larval phase (Leis, 2007). In addition, the use of proper information on ELTs (i.e. spawning dates, propagule larval duration), gathered at the same spatial and temporal context of the oceanographic data, allowed us to improve the accuracy of the simulated dispersal.

The spatial scale of dispersal recorded here is in accordance with the estimation obtained from otolith chemical analysis of *O. melanura* for the same spatial and temporal context (Calò et al., 2016). Results from dispersal simulations showed that dispersal distance depended mainly on spatial factors. The geographical position of release zones was also found responsible of larval dispersal distance variability in other recent works (Treml et al., 2015) (Thomas et al., 2014). In our study, propagules released in the centre of the study area (Cabo de Palos MPA) dispersed twice further than those released in the northern and southern zones, probably due to the oceanographic characteristics of the region. The northern half of the study area is characterised by an extended continental shelf (~300 km from the coast) and shallow waters (0 - 200m). In the southern sector the continental shelf is very narrow and the continental slope, cut through by a series of coastal canyons, is only few thousands of meters distant from the coast (Calvin Calvo et al., 1999). Cabo de Palos marine reserve is geographically located in the transition between these two morphologically different areas and the oceanographic circulation in its surroundings reflects these geomorphological features, determining strong currents compared to the northward and southward coastal sectors of the study area. This pattern was clearly highlighted by averaging current velocities in the study area over the time window in which simulations were run (i.e. 21st June 2013 – 15th July 2013) (Fig. 6, 1-4). From this point of view, the southward shift in the distribution of settled propagules released from zone L5 (i.e. Cabo e Palos MPA) reported above, could be a consequence of the strong current dynamic characterising the area around Cabo de Palos (Fig 6, 1-4). Variability in dispersal distance also depended on the depth range of propagule release, since

390   particles released in shallow waters dispersed less in average than those released deeper in the 3

391   release zones considered. This outcome contradicts the general assumption that current velocities

392   tend to decrease with depth. However, the particular oceanographic conditions characterising the

393   study area are likely responsible for this dispersal pattern, with deeper waters moving faster than

394   shallow ones (Fig. 6, a and b). This difference is probably due to coastal recirculation

395   characteristics, for example the formation of coastal eddies. These oceanographic features are

396   related to wind forcing and are consequently more pronounced at the surface than in deeper water

397   layers. The analysis of model runs with different release depths shows that the formation of a

398   relatively wide recirculation system trapped a large number of particles close to the surface, while

399   particles released in deeper water were only partially affected by the eddy and followed longer paths

400   southward (Fig. 7). Considering the significant influence of depth on propagule dispersal distances,

401   any biological process may be important to be considered in future work. From this perspective, the

402   collection of information on egg buoyancy, larval behaviour and movement of the saddled sea

403   bream would allow to improve the simulations run in this study.

404   The significant variability in dispersal distances due to spatial factors could have blurred the effect

405   of dispersal duration, here found non-significant. Although the relation between propagule dispersal

406   and its duration in the pelagic environment is currently a matter of debate (Shanks, 2009) (Leis et

407   al., 2013), it is generally accepted that fish dispersal distance is positively correlated with dispersal

408   duration. In this work, however, the relatively short time of dispersal and the small difference

409   between the two dispersal durations (2.5 days) could have determined the lack of significant

410   variability of the temporal factor. Moreover, the frequent occurrence of small and medium-size

411   coastal eddies along the study area could have contributed to the observed result. Propagules that

412   enter an eddy could remain trapped inside it, blurring the effects of different dispersal times. The

413   variability of propagule dispersal in this geographical context and associated with the depth of

414   release suggests that even for species with a short propagule dispersal phase (~14 days in the case

415   of *O. melanura*), local differences in oceanographic conditions can lead to a wide range of dispersal

416   outcomes.

417   Information on the location of fish spawning grounds and the scale of dispersal is crucially

418   important for elucidating connectivity patterns between populations, and for providing the optimal

419   background knowledge in order to design efficient protection and management strategies. The

420   method used here, combining model simulations with information on natal origin composition

421   resulting from otolith chemical analysis, supported by accurate information on fish biological traits,

422   is a first attempt to locate fish release zones in the Mediterranean Sea. The approach implemented

423   could provide valuable results for the localization of fish spawning grounds for other species,

424   especially considering the current lack of methodological alternatives for addressing this issue

425   worldwide.

426

427   ACKNOWLEDGMENTS

431 Andrello, M., Guilhaumon, F., Albouy, C., Parravicini, V., Scholtens, J., Verley, P., Barange, M.,
432   Sumaila, U.R., Manel, S., Mouillot, D., 2017. Global mismatch between fishing dependency
433   and larval supply from marine reserves. Nat. Commun. doi:10.1038/ncomms16039

434 Andrello, M., Jacobi, M.N., Manel, S., Thuiller, W., Mouillot, D., 2015a. Extending networks of
435   protected areas to optimize connectivity and population growth rate. Ecography (Cop.). 38,
436   273–282. doi:10.1111/ecog.00975

437 Andrello, M., Mouillot, D., Beuvier, J., Albouy, C., Thuiller, W., Manel, S., 2013. Low connectivity
438   between Mediterranean marine protected areas: a biophysical modeling approach for the dusky
439   grouper Epinephelus marginatus. PLoS One 8, e68564. doi:10.1371/journal.pone.0068564

440 Andrello, M., Mouillot, D., Somot, S., Thuiller, W., Manel, S., 2015b. Additive effects of climate
441   change on connectivity between marine protected areas and larval supply to fished areas.
442   Divers. Distrib. 21, 139–150. doi:10.1111/ddi.12250

443 Aspillaga, E., Bartumeus, F., Linares, C., Starr, R.M., López-sanz, À., Díaz, D., Zabala, M., Hereu,
444   B., 2016. Ordinary and Extraordinary Movement Behaviour of Small Resident Fish within a
445   Mediterranean Marine Protected Area. PLoS One 11, 1–19. doi:10.6084/m9.figshare.3188587

446 Barbee, N., Swearer, S., 2007. Characterizing natal source population signatures in the diadromous
447   fish Galaxias maculatus, using embryonic otolith chemistry. Mar. Ecol. Prog. Ser. 343, 273–
448   282. doi:10.3354/meps06886

449 Boomhower, J.P., Romero, M. a, Posada, J.M., Kobara, S., Heyman, W.D., 2007. Identification of
450   Reef Fish Spawning Aggregation Sites in Los Roques Archipelago National Park , Venezuela.
451   Proc. 60th Gulf Caribb. Fish. Inst.

452 Burgess, S.C., Baskett, M.L., Grosberg, R.K., Morgan, S.G., Strathmann, R.R., 2015. When is
453   dispersal for dispersal? Unifying marine and terrestrial perspectives. Biol. Rev. n/a-n/a.
454   doi:10.1111/brv.12198

455 Calò, A., Di Franco, A., De Benedetto, G., Pennetta, A., Pérez-Ruzafa, Á., García-Charton, J., 2016.
456   Propagule dispersal and larval patch cohesiveness in a Mediterranean coastal fish. Mar. Ecol.
457   Prog. Ser. 544, 213–224. doi:10.3354/meps11609

458 Calò, A., Félix-Hackradt, F.C., Garcia, J., Hackradt, C.W., Rocklin, D., Treviño Otón, J., Charton, J.
459   a. G., 2013. A review of methods to assess connectivity and dispersal between fish populations
460   in the Mediterranean Sea. Adv. Oceanogr. Limnol. 4, 150–175.
461   doi:10.1080/19475721.2013.840680

462 Calvin Calvo, J.C., Franco Navarra, I., Marín Atucha, A., Belmonte Ríos, A., Ruiz Fernandez, J.M.,
463   1999. El litoral sumergido de la region de murcia. Cartografía bionómica y valores
464   ambientales.

465 Cowen, R.K., 2007. Population Connectivity in Marine Systems. Oceanography 20, 14–21.
466   doi:10.1126/science.1122039

467 Di Franco, A., Calò, A., Pennetta, A., De Benedetto, G., Planes, S., Guidetti, P., 2015. Dispersal of
468   larval and juvenile seabream: Implications for Mediterranean marine protected areas. Biol.
469   Conserv. 192, 361–368. doi:10.1016/j.biocon.2015.10.015

470   Green, A.L., Maypa, A.P., Almany, G.R., Rhodes, K.L., Weeks, R., Abesamis, R. a., Gleason, M.G.,
471   Mumby, P.J., White, A.T., 2014. Larval dispersal and movement patterns of coral reef fishes,
472   and implications for marine reserve network design. Biol. Rev. 90, 1215–1247.
473   doi:10.1111/brv.12155

474   Grüss, A., Kaplan, D.M., Guénette, S., Roberts, C.M., Botsford, L.W., 2011. Consequences of adult
475   and juvenile movement for marine protected areas. Biol. Conserv. 144, 692–702.
476   doi:10.1016/j.biocon.2010.12.015

477   Heyman, W.D., Azueta, J., Lara, O., Majil, I., Neal, D., Luckhurst, B., Paz, M., Morrison, I.,
478   Rhodes, K.L., Kjerve, B., Wade, B., Requena, N., 2004. Protocolo para el monitoreo de
479   agregaciones reproductivas de peces arrecifales en el Arrecife Mesoamericano y el Gran
480   Caribe.

481   Juza, M., Mourre, B., Renault, L., Gómara, S., Sebastian, K., López, S.L., Borrueco, B.F., Beltran,
482   J.P., Troupin, C., Tomás, M.T., Heslop, E., Casas, B., Tintoré, J., 2016. Operational SOCIB
483   forecasting system and multi-platform validation in the Western Mediterranean. J. Oper.
484   Oceanogr. 9231. doi:10.1002/2013JC009231.

485   Leis, J., 2007. Behaviour as input for modelling dispersal of fish larvae: behaviour, biogeography,
486   hydrodynamics, ontogeny, physiology and phylogeny meet hydrography. Mar. Ecol. Prog. Ser.
487   347, 185–193. doi:10.3354/meps06977

488   Leis, J.M., 2015. Is dispersal of larval reef fishes passive?, in: Mora, C. (Ed.), Ecology of Fishes on
489   Coral Reefs. Cambridge University Press, pp. 223–226.

490   Leis, J.M., Caselle, J.E., Bradbury, I.R., Kristiansen, T., Llopiz, J.K., Michael, J., O'Connor, M.I.,
491   Paris, C.B., Shanks, A.L., Sogard, S.M., Swearer, S.E., Treml, E.A., Vetter, R.D., Warner, R.R.,
492   2013. Does fish larval dispersal differ between high and low latitudes ? Proc. R. Soc. Biol. Sci.
493   280.

494   Leis, J.M., van Herwerden, L., Patterson, H.M., 2011. Estimating connectivity in marine fish
495   populations: what works best?, in: Oceaography and Marine Biology: An Annual Review. pp.
496   193–234.

497   Lett, C., Ayata, S.-D., Huret, M., Irisson, J., 2010. Biophysical modelling to investigate the effects
498   of climate change on marine population dispersal and connectivity. Prog. Oceanogr. 87, 106–
499   113.

500   Lett, C., Verley, P., Mullon, C., Parada, C., Brochier, T., Penven, P., Blanke, B., 2008. A Lagrangian
501   tool for modelling ichthyoplankton dynamics. Environ. Model. Softw. 23, 1210–1214.
502   doi:10.1016/j.envsoft.2008.02.005

503   Lozano Quijada, F., Ramos-Esplá, A.A., 2015. Nueva Tabarca, un desafío multidisciplnar.

504   Millot, C., 1999. Circulation in the Western Mediterranean Sea. J. Mar. Syst. 20, 423–442.
505   doi:10.1016/S0924-7963(98)00078-5

506   Nakata, H., Kimura, S., Okazaki, Y., Kasai, A., 2000. 120042 Implications of meso-scale eddies
507   caused by frontal disturbances of the Kuroshio Current for anchovy recruitment. J. Mar. Sci.
508   57, 143–152. doi:10.1006/jmsc.1999.0565

509 Ospina-Álvarez, A., Bernal, M., Catalán, I.A., Roos, D., Bigot, J.L., Palomera, I., 2013. Modeling
510   Fish Egg Production and Spatial Distribution from Acoustic Data: A Step Forward into the
511   Analysis of Recruitment. PLoS One 8, 1–18. doi:10.1371/journal.pone.0073687

512 Ospina-Alvarez, A., Catalán, I. a., Bernal, M., Roos, D., Palomera, I., 2015. From egg production to
513   recruits: Connectivity and inter-annual variability in the recruitment patterns of European
514   anchovy in the northwestern Mediterranean. Prog. Oceanogr. 138, 431–447.
515   doi:10.1016/j.pocean.2015.01.011

516 R Development Core Team, 2013. R: A Language and Environment for Statistical Computing, R
517   Foundation for Statistical Computing Vienna Austria.

518 Ramos-Esplá, A., 1985. Tabarca, La reserva marina de la Isla Plana o Nueva.

519 Sabatés, A., Olivar, M.P., Salat, J., Palomera, I., Alemany, F., 2007. Physical and biological
520   processes controlling the distribution of fish larvae in the NW Mediterranean. Prog. Oceanogr.
521   74, 355–376. doi:10.1016/j.pocean.2007.04.017

522 Sabatés, A., Salat, J., Raya, V., Emelianov, M., 2013. Role of mesoscale eddies in shaping the
523   spatial distribution of the coexisting Engraulis encrasicolus and Sardinella aurita larvae in the
524   northwestern Mediterranean. J. Mar. Syst. 111–112, 108–119.
525   doi:10.1016/j.jmarsys.2012.10.002

526 Sánchez-Lisazo, J.L., 1993. Estudio de la pradera de Posidonia oceanica (L.) Delile de la reserva
527   marina de Tabarca (Alicante): Fenología y producción primaria. Dep. Ciències Ambient. i
528   Recur. Nat.

529 Shanks, A.L., 2009. Pelagic Larval Duration and Dispersal Distance Revisited. Biol. Bull. 216,
530   373–385.

531 Shchepetkin, A.F., McWilliams, J.C., 2005. The regional oceanic modeling system (ROMS): a split-
532   explicit, free-surface, topography-following-coordinate oceanic model. Ocean Model. 9, 347–
533   404. doi:10.1016/j.ocemod.2004.08.002

534 Shulzitski, K., Sponaugle, S., Hauff, M., Walter, K., D'Alessandro, E.K., Cowen, R.K., 2015. Close
535   encounters with eddies: oceanographic features increase growth of larval reef fishes during
536   their journey to the reef. Biol. Lett. 11, 20140746. doi:10.1098/rsbl.2014.0746

537 Tanner, S.E., Teles-machado, A., Martinho, F., Peliz, Á., Cabral, H.N., 2017. Modelling larval
538   dispersal dynamics of common sole (Solea solea) along the western Iberian coast. Prog.
539   Oceanogr. 156, 78–90. doi:10.1016/j.pocean.2017.06.005

540 Thomas, Y., Dumas, F., Andréfouët, S., 2014. Larval dispersal modeling of pearl oyster pinctada
541   margaritifera following realistic environmental and biological forcing in ahe atoll lagoon.
542   PLoS One 9. doi:10.1371/journal.pone.0095050

543 Thorrold, S., Zacherl, D., Levin, L., 2007. Population Connectivity and Larval Dispersal Using
544   Geochemical Signatures in Calcified Structures. Oceanography 20, 80–89.
545   doi:10.5670/oceanog.2007.31

546 Thorrold, S.R., Latkoczy, C., Swart, P.K., Jones, C.M., 2001. Natal homing in a marine fish

547   metapopulation. Science 291, 297–9. doi:10.1126/science.291.5502.297

548   Treml, E.A., Ford, J.R., Black, K.P., Swearer, S.E., 2015. Identifying the key biophysical drivers,
549   connectivity outcomes, and metapopulation consequences of larval dispersal in the sea. Mov.
550   Ecol. 3, 17. doi:10.1186/s40462-015-0045-6

551   Watson, J.R., Mitarai, S., Siegel, D.., Caselle, J.E., Dong, C., McWilliams, J.C., 2010. Realized and
552   potential larval connectivity in the Southern California Bight. Mar. Ecol. Prog. Ser. 401, 31–
553   48. doi:10.3354/meps08376

554   Werner, F.E., Cowen, R.K., Paris, C.B., 2007. Coupled biological and physical models: present
555   capabilities and necessary developments for future studies of population connectivity.
556   Oceanography 20, 54–69.

557
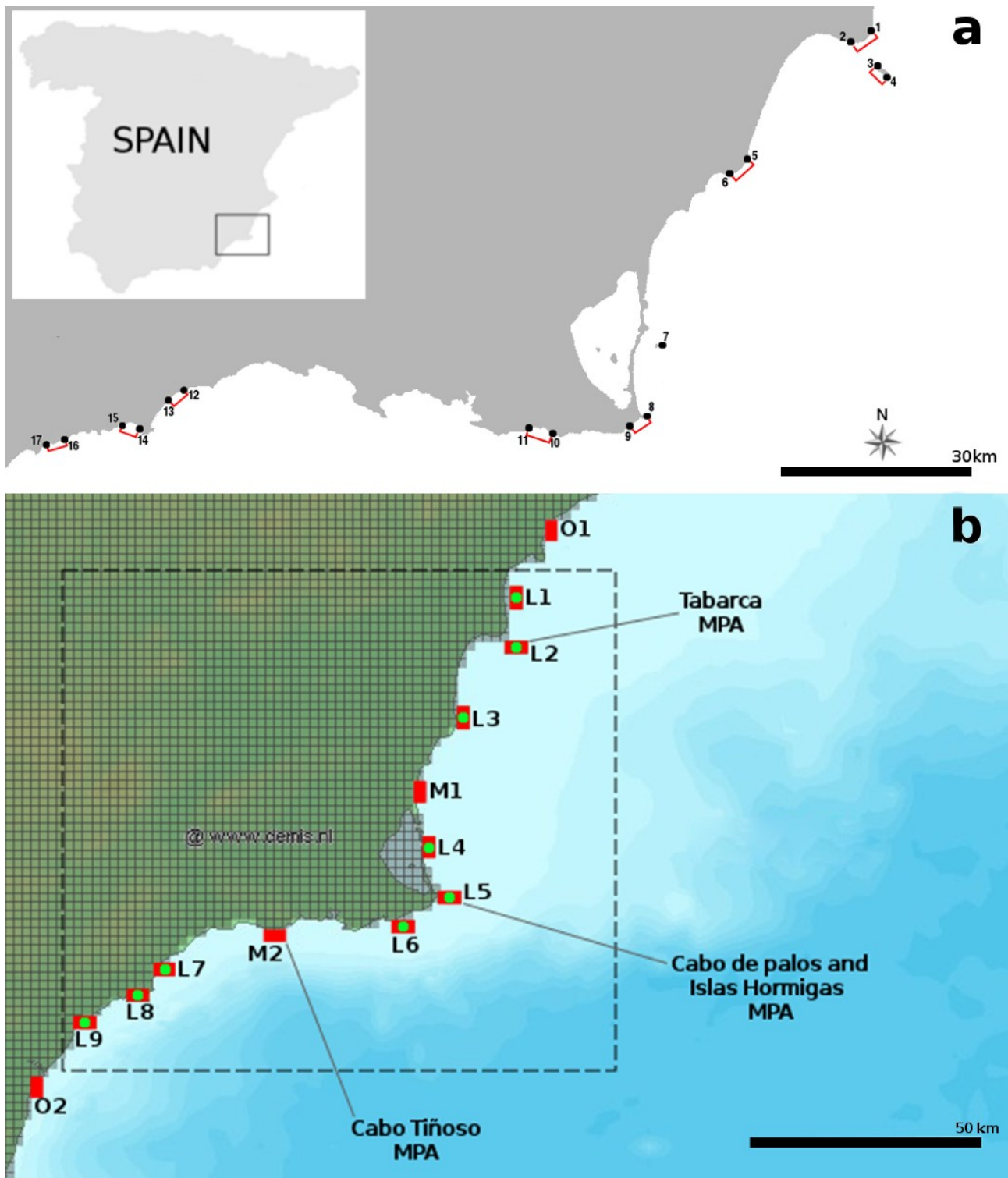
Figure 1. a) Study area considered in the work on otolith chemical analysis (Calò et al., 2016): black dots represent the 17 sites sampled, red segments link pairs of sites pooled for creating the 'pooled locations' used in the present study; b) Domain considered in simulations: red rectangles represent the 13 potential release zones used, green dots mark the 9 settlement zones representing the 'pooled locations' shown in (a); the dashed rectangle encloses the study area shown in (a). Zones L2, L5, and M2 include Marine Protected Areas (MPAs).
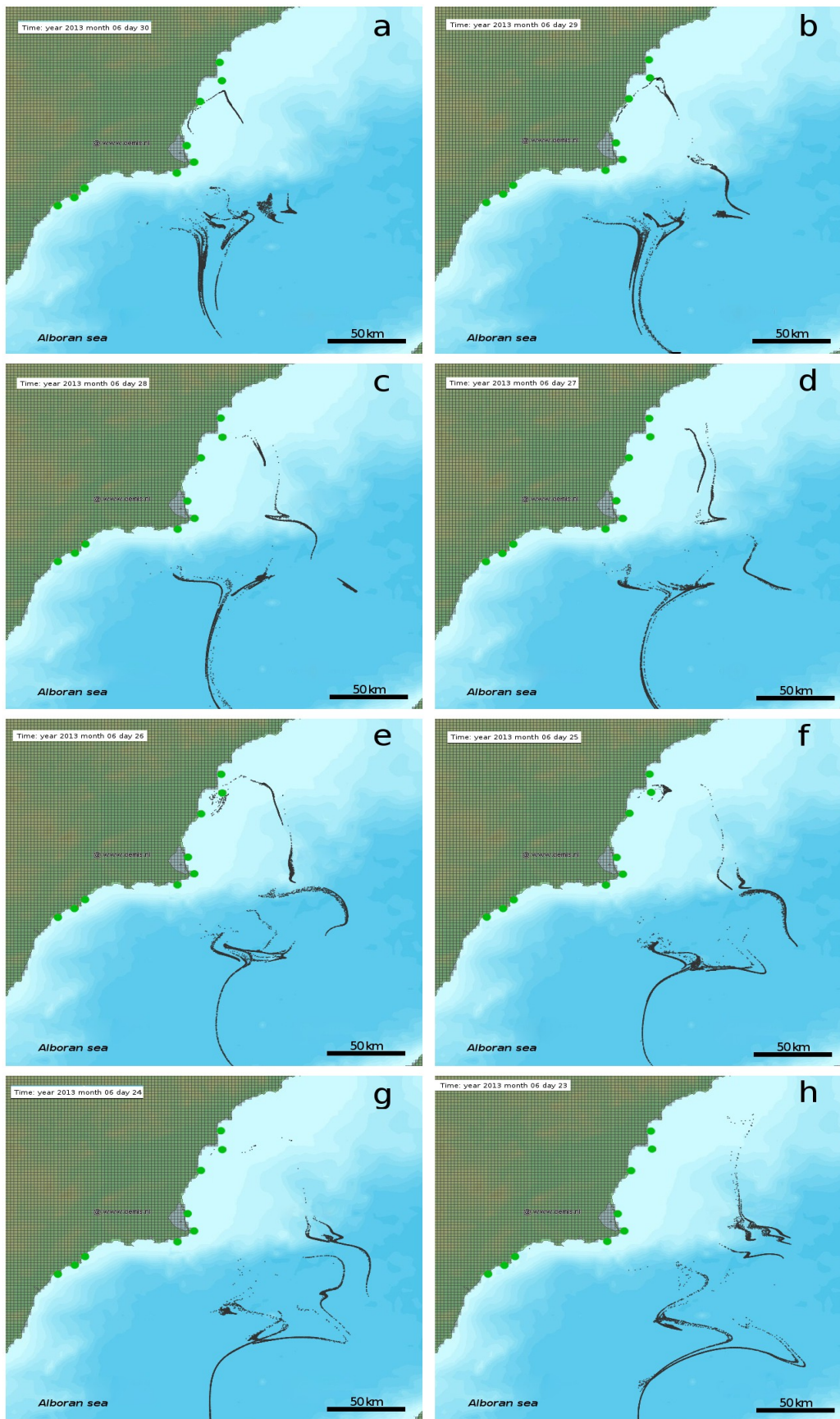
Figure 2. Dispersal patterns obtained from backtracking simulations. Each panel represents the final step of each of the 8 simulations run backward with a different release date: from July 14th (a) to July 7th (h). Black dots represent simulated propagules. Green dots represent release zones.

Figure 3. Percentage of *O. melanura* settlers/particles from natal origin/release zone. a) Results from otolith chemical analysis: settler distribution in the 9 'pooled locations' from the 5 major natal
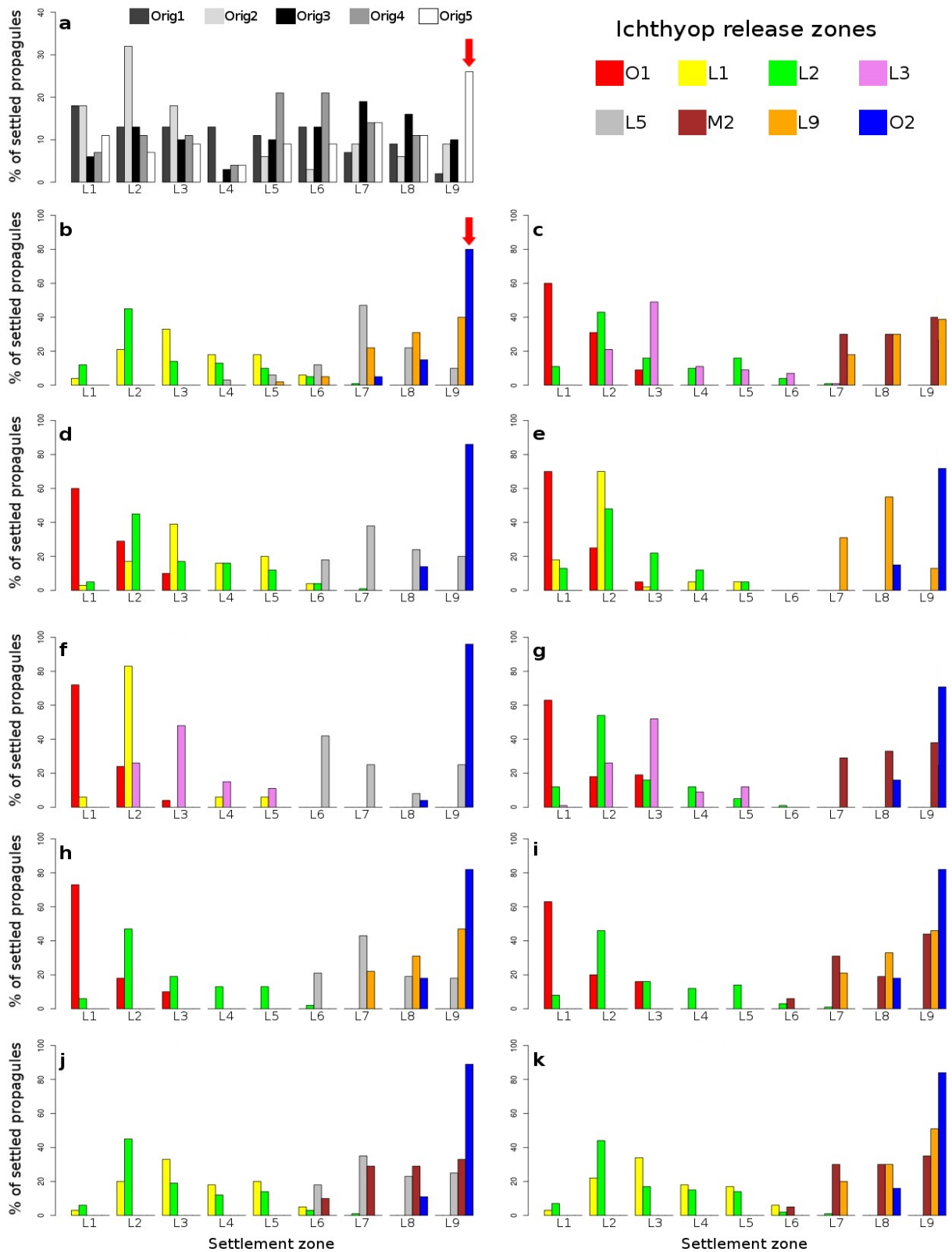
origins (grey scale) identified by (Calò et al., 2016); as an example, the white bar indicated by the red arrow shows that ~ 30% of the propagules identified from unknown origin 5 were collected in zone L9; b)-k) Propagule distributions in the 9 settlement zones as resulted from larval dispersal

573   simulations using different sets of release zones (here taken as putative spawning areas, i.e., the red

574   rectangles in Fig. 1b). Only simulated propagule distributions that were significantly correlated with

575   the distribution obtained from otolith chemical analysis (panel a) are shown (See Tab. S2 for

576   details). As an example, the blue bar indicated by the red arrow in panel b shows that ~ 80% of the

577   individuals released in zone O2 settled in zone L9
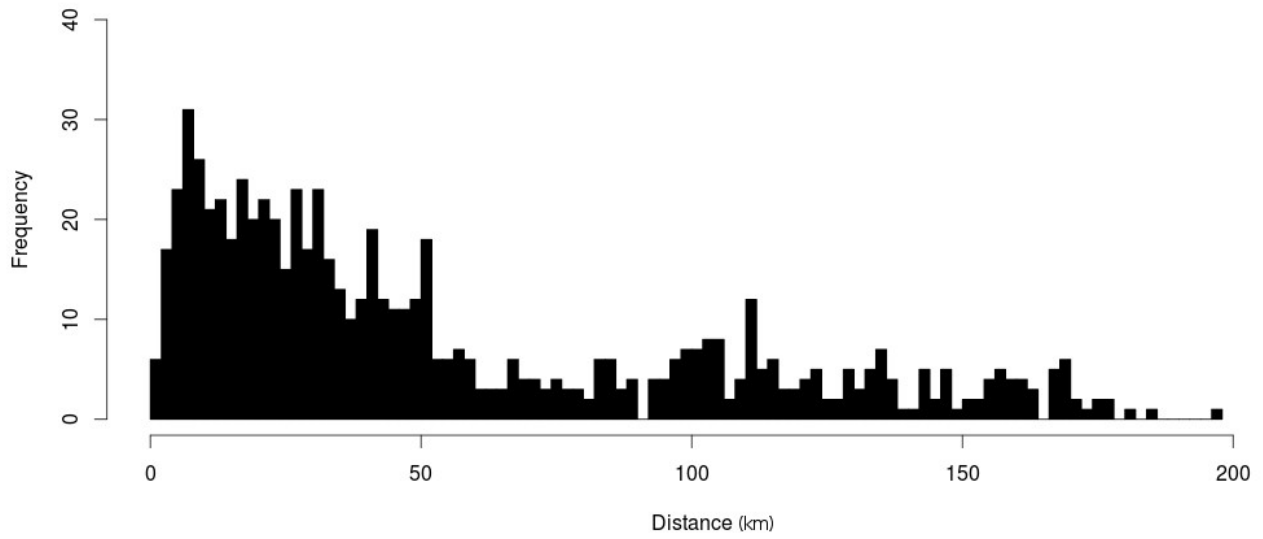
579 Figure 4. Frequency distribution of dispersal distances obtained for *O. melanura* from all
580 simulations.

Source	Df	SS	Fvalue	
T	1	2.63	3.027	
D	3	72.63	8.41	*
Z	2	177.76	146.975	***
T*D	3	2.7	1.64	
T*Z	2	1.73	1.434	
D*Z	6	17.27	4.76	***
T*D*Z	6	3.29	0.908	
Residual	696	420.89		

581   Table 1. ANOVA on dispersal distances: Df=degrees of freedom, SS= sum of squares, T=dispersal

582   duration, D=release depth range, Z=release zone, *=p<0.05, ***=p<0.001.
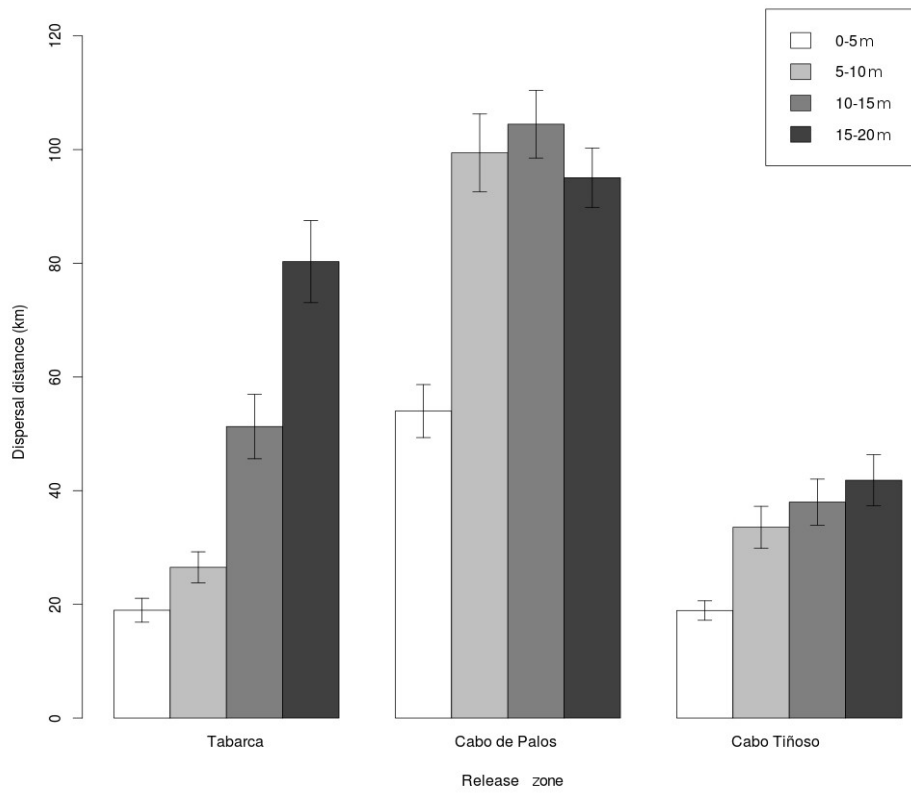
583   Figure 5. Dispersal distance (mean ± SE) for all combinations of release zone and release depth
584   range.
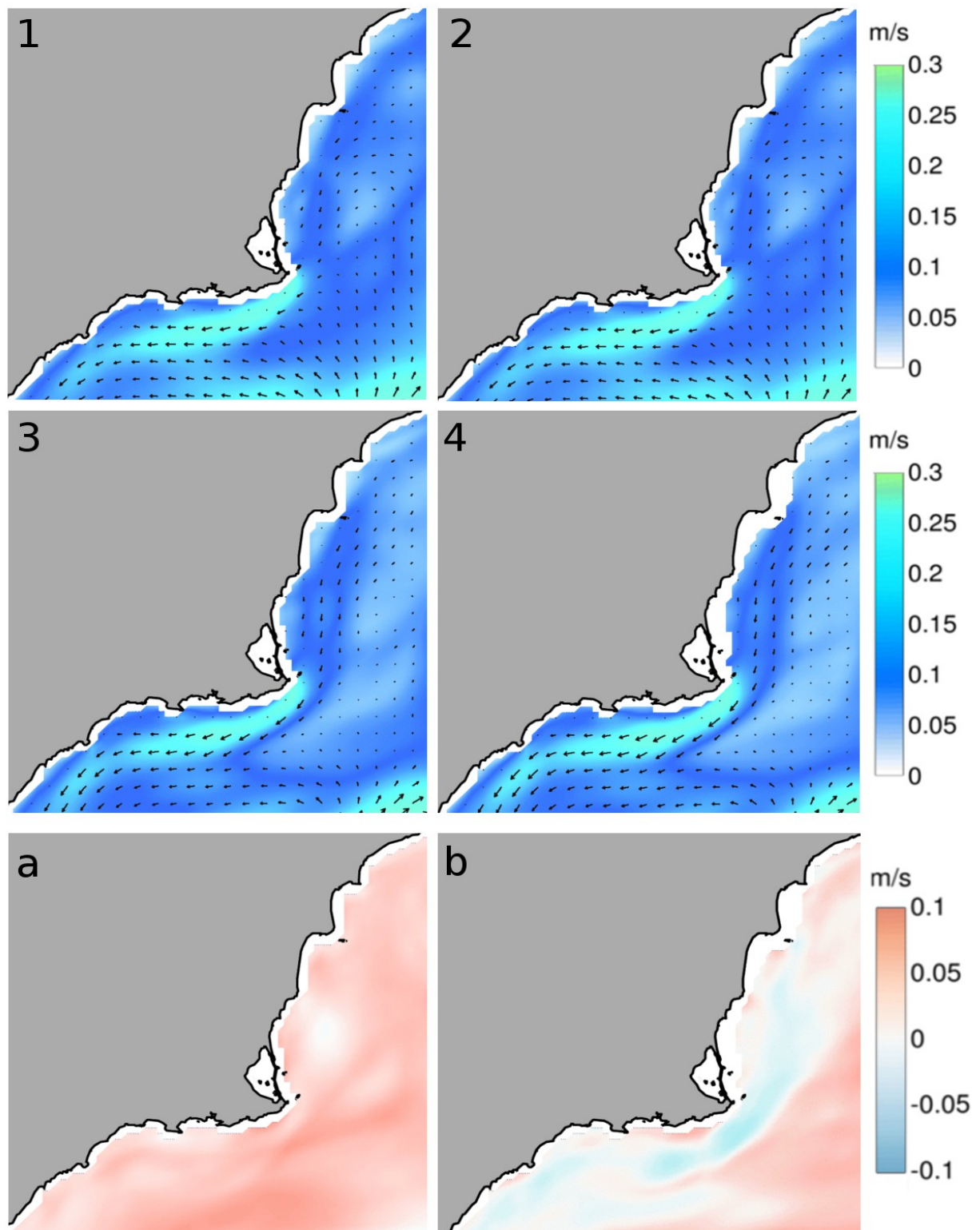
Figure 6. (1-4) Maps of average current velocities over the simulation period June 21st – July 15th 2013 at different depth: 5 m (1), 10 m (2), 15 m (3) and 20 m (4). (a and b) Maps of difference in average current velocity between 0 m and 10 m (a) and between 10 m and 20 m (b) over the same time period: positive values (red colours) indicate that currents at the upper layer were faster than deeper currents; negative values (blue colours) indicate the opposite.
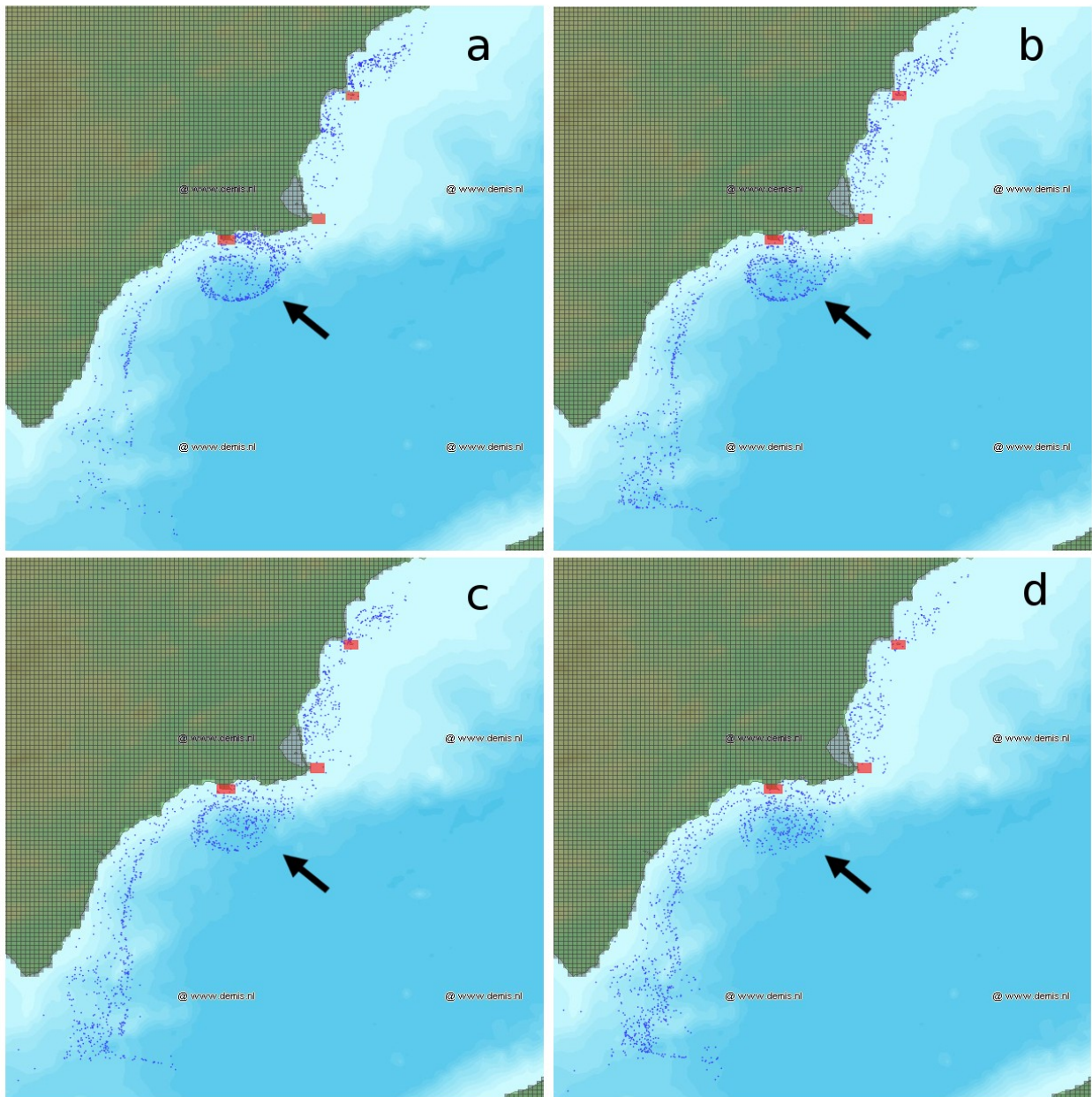
Fig 7. Last steps of larval dispersal simulations from 3 release zones (MPAs, red rectangles) and daily release from June 21st to July 2nd. Each panel corresponds to a different release depth: 5 m (a), 10 m (b), 15 m (c) and 20 m (d). Black arrows indicate the position of one of the coastal eddies responsible of particle trapping in shallower waters. Note the decreasing density of particles inside the eddy and the increasing abundance of particles in the south of the domain from (a) to (d).

Ichthyop run	Release zones 1	2	3	4	5	Mantel's test	pvalue	Ichthyop Run	Release zones 1	2	3	4	5	Mantel's Test	pvalue
1	O1	L2	M1	M2	O2	0.3436	0.1191	26	L2	L5	M2	L9	O2	0.455	0.0505
2	L3	M1	L6	L9	O2	0.0721	0.4377	27	L1	M1	L6	L7	L8	-0.3424	0.9102
3	L1	L2	L5	L9	O2	0.496	0.0381	28	O1	L2	L3	M2	L9	0.428	0.0313
4	O1	L2	L5	M2	O2	0.4435	0.056	29	L1	L3	M1	L6	L8	-0.3115	0.8969
5	L1	M1	L6	L9	O2	0.0932	0.418	30	L1	L3	M1	L4	L9	-0.1929	0.7006
6	L2	M1	L5	L6	L9	-0.0785	0.5457	31	L1	L2	L5	L8	O2	0.3561	0.1078
7	O1	L4	M2	L8	O2	0.2379	0.2013	32	M1	L5	L6	L7	O2	-0.0554	0.5673
8	L1	L5	L6	M2	L7	-0.1127	0.6623	33	L1	L2	L3	M2	L7	0.078	0.3683
9	L1	L3	M1	L4	L8	-0.3411	0.9044	34	L5	L6	M2	L7	L9	0.0607	0.3873
10	O1	L1	M1	L4	L5	-0.2326	0.7645	35	L1	L3	M1	L7	O2	0.0037	0.4877
11	O1	L1	L3	L6	M2	-0.081	0.5805	36	L3	L4	L7	L9	O2	0.1683	0.2804
12	O1	L2	L3	L4	L7	-0.1017	0.6317	37	O1	L2	L3	M1	L6	-0.1062	0.5975
13	O1	L3	L4	L5	M2	0.0764	0.3799	38	O1	L2	L5	L6	L7	-0.0202	0.5068
14	L1	L3	M1	L5	L6	-0.2409	0.8184	39	L1	L3	L6	L7	O2	0.2136	0.2255
15	L1	L4	L5	L9	O2	0.2395	0.1954	40	L2	L4	L7	L8	L9	0.1435	0.285
16	O1	L1	L4	L7	L8	-0.0748	0.6087	41	L1	L2	L4	L5	M2	0.2217	0.1865
17	L1	L2	M1	L5	L9	-0.0378	0.4597	42	L2	M2	L7	L9	O2	0.3952	0.0832
18	L2	L3	M2	L7	O2	0.3344	0.1346	43	O1	L1	M2	L8	O2	0.2395	0.192
19	O1	L1	L3	M1	L7	-0.2599	0.7963	44	O1	L4	L5	L6	L8	0.1763	0.2584
20	O1	L2	L6	L7	L8	0.0212	0.4575	45	L1	L2	L3	M1	M2	0.0204	0.386
21	O1	L2	M1	L4	M2	-0.0833	0.5823	46	L4	L5	L6	L6	M2	-0.068	0.597
22	L1	L3	L4	L7	L9	-0.1178	0.6695	47	L1	L4	L5	L6	O2	0.2415	0.1865
23	O1	M1	L7	L9	O2	0.0043	0.4801	48	L1	L2	L3	L6	M2	0.205	0.1882
24	L1	L2	L3	L4	L9	0.116	0.3171	49	L1	L2	L3	L4	L8	-0.1286	0.6768
25	L3	L4	L5	M2	L8	-0.0635	0.5914	50	L3	M1	L5	L7	L8	-0.3173	0.8755

Table S1. Results from the first set of (50) Mantel's correlations between the settler distribution obtained from otolith chemical analysis and the ones obtained from Ichthyop simulations. Rows highlighted in red indicate significant Mantel's correlation.

Ichthyop Run	1	2	3	4	5	Mantel's Test	pvalue	Ichthyop Run	1	2	3	4	5	Mantel's Test	pvalue
1*	L1	L2	L5	L9	O2	0.496	0.0366	29	O1	L2	L3	L9	O2	0.4319	0.0715
2*	O1	L2	L3	M2	L9	0.428	0.0305	30	O1	L2	L5	M2	L9	0.3033	0.0935
3	L2	L5	M2	L9	O2	0.455	0.0508	31	O1	L2	L5	L9	O2	0.4746	0.0493
4	O1	L2	L5	M2	O2	0.4435	0.0553	32	O1	L2	M2	L9	O2	0.5395	0.0263
5	O1	L1	L2	L3	L5	0.1256	0.3005	33	O1	L3	L5	M2	L9	0.0299	0.4113
6	O1	L1	L2	L3	M2	0.0746	0.3724	34	O1	L3	L5	M2	O2	0.3119	0.1431
7	O1	L1	L2	L3	L9	0.2909	0.1248	35	O1	L3	L5	L9	O2	0.2819	0.1525
8	O1	L1	L2	L3	O2	0.456	0.0572	36	O1	L3	M2	L9	O2	0.2654	0.168
9	O1	L1	L2	L5	M2	0.2317	0.2046	37	O1	L5	M2	L9	O2	0.3146	0.1343
10	O1	L1	L2	L5	L9	0.2925	0.1147	38	L1	L2	L3	L5	M2	0.1105	0.3186
11	O1	L1	L2	L5	O2	0.5526	0.0218	39	L1	L2	L3	L5	L9	0.1623	0.2381
12	O1	L1	L2	M2	L9	0.3055	0.1093	40	L1	L2	L3	L5	O2	0.4348	0.0713
13	O1	L1	L2	M2	O2	0.4011	0.0788	41	L1	L2	L3	M2	L9	0.1774	0.2359
14	O1	L1	L2	L9	O2	0.5974	0.0147	42	L1	L2	L3	M2	O2	0.4319	0.0784
15	O1	L1	L3	L5	M2	-0.019	0.4882	43	L1	L2	L3	L9	O2	0.4416	0.0708
16	O1	L1	L3	L5	L9	0.0423	0.4072	44	L1	L2	L5	M2	L9	0.2966	0.0891
17	O1	L1	L3	L5	O2	0.6271	0.0129	45	L1	L2	L5	M2	O2	0.5146	0.0235
18	O1	L1	L3	M2	L9	0.2089	0.2019	46	L1	L2	M2	L9	O2	0.4851	0.0407
19	O1	L1	L3	M2	O2	0.297	0.1496	47	L1	L3	L5	M2	L9	-0.0696	0.5995
20	O1	L1	L3	L9	O2	0.415	0.0865	48	L1	L3	L5	M2	O2	0.2664	0.1912
21	O1	L1	L5	M2	L9	0.1425	0.268	49	L1	L3	L5	L9	O2	0.2682	0.2013
22	O1	L1	L5	M2	O2	0.4267	0.0778	50	L1	L3	M2	L9	O2	0.2645	0.2013
23	O1	L1	L5	L9	O2	0.3236	0.1096	51	L1	L5	M2	L9	O2	0.3161	0.1745
24	O1	L1	M2	L9	O2	0.333	0.116	52	L2	L3	L5	M2	L9	0.3097	0.0897
25	O1	L2	L3	L5	M2	0.2502	0.1466	53	L2	L3	L5	M2	O2	0.4394	0.0675
26	O1	L2	L3	L5	L9	0.1346	0.3001	54	L2	L3	L5	L9	O2	0.4645	0.0566
27	O1	L2	L3	L5	O2	0.4198	0.0628	55	L2	L3	M2	L9	O2	0.4199	0.0795
28	O1	L2	L3	M2	O2	0.5687	0.0158	56	L3	L5	M2	L9	O2	0.3146	0.1821

Table S2. Results from the second set of (56) Mantel's correlations between the settler distribution obtained from otolith chemical analysis and the ones obtained from Ichthyop simulations. Rows highlighted in red indicate significant Mantel's correlation. The sign '*' indicates the two runs resulted statistically significant in the previous analysis.